Supplementary Information for:

Inner ear sensory system changes as extinct crocodylomorphs transitioned from land to water

Julia A. Schwab[a,*], Mark T. Young[a], James M. Neenan[b], Stig A. Walsh[a,c], Lawrence M. Witmer[d], Yanina Herrera[e], Ronan Allain[f], Christopher A. Brochu[g], Jonah N. Choiniere[h], James M. Clark[i], Kathleen N. Dollman[h,j], Steve Etches[k], Guido Fritsch[l], Paul M. Gignac[m], Alexander Ruebenstahl[n], Sven Sachs[o], Alan H. Turner[p], Patrick Vignaud[q], Eric W. Wilberg[p], Xu Xing[r], Lindsay E. Zanno[s,t] & Stephen L. Brusatte[a,c]

[a]School of GeoSciences, Grant Institute, James Hutton Road, The King's Buildings, University of Edinburgh, Edinburgh, EH9 3FE, UK; [b]Oxford University Museum of Natural History, Oxford, OX1 3PW, United Kingdom; [c] Department of Natural Sciences, National Museum of Scotland, National Museum of Scotland, Chambers Street, Edinburgh, EH 1 1JF, UK; [d]Department of Biomedical Sciences, Heritage College of Osteopathic Medicine, Ohio University, Athens, Ohio 45701, USA; [e]Consejo Nacional de Investigaciones Científicas y Técnicas, División Paleontología Vertebrados, Museo de La Plata, FCNyM, UNLPNational University of La Plata, La Plata, Argentina; [f] Centre de Recherche sur la Paléobiodiversité et les Paléoenvironnements, Muséum National d'Histoire Naturelle, CP 38, 8 rue Buffon, 75005 Paris, France; [g]Department of Earth and Environmental Sciences, University of Iowa, Iowa City, Iowa 52242, USA; [h]Evolutionary Studies Institute, University of the Witwatersrand, Johannesburg 2000, South Africa; [i]Department of Biological Sciences, George Washington University, Washington DC 20052, USA; [j]School of Geosciences, University of the Witwatersrand, Johannesburg 2000, South Africa;

www.pnas.org/cgi/doi/10.1073/pnas.2002146117

[k]Museum of Jurassic Marine Life, Kimmeridge, BH20 5PE, UK; [l]Department of Reproduction Management, Leibniz Institute for Zoo and Wildlife Research, 10315 Berlin, Germany; [m]Department of Anatomy and Cell Biology, Oklahoma State University Center for Health Sciences, Tulsa, Oklahoma 74107, USA; [n]Department of Geology and Geophysics, Yale University, New Haven, CT 06511, USA; [o]Abteilung Geowissenschaften, Naturkunde-Museum Bielefeld, Naturkunde-Museum Bielefeld, Abteilung Geowissenschaften, Adenauerplatz 2, 33602 Bielefeld, Germany; [p]Department of Anatomical Sciences, Stony Brook University, Stony Brook, New York 11794, USA; [q] Laboratoire de Paléontologie, Evolution, Paléoécosystèmes et Paléoprimatologie, CNRS UMR 7262, Department of Geosciences, University of Poitiers, France; [r]Institute of Vertebrate Paleontology & Paleoanthropology, Chinese Academy of Sciences, Beijing, China; [s]Paleontology, North Carolina Museum of Natural Sciences, Raleigh, NC 27601, USA; [t]Department of Biological Sciences, North Carolina State University, Raleigh, NC 27695, USA

* Correspondence: julia.schwab@ed.ac.uk

1. Specimens Examined

Table S1. Detailed information on the specimens we scanned; their museum specimen numbers, ages, and CT scanning parameters. The abbreviations are the notions used in the Figures in the main text and the Supplementary Tables.

Taxa	ID	Abbr.	voxel size (mm)	facility
Junggarsuchus sloani	IVPP V14010	JuSl	0.13	Institute of Vertebrate Paleontology and Paleoanthropology (IVPP) of the Chinese Academy of Sciences
Undescribed sphenosuchian	NCSM 21722	UnSp	0.039327	Nikon XTH 225 ST µCT scanner, Shared Materials Instrumentation Facility, Duke University, Durham, NC
Eopneumatosuchus colberti	MNA V2460	EoCo	0.092	General Electric eXplore Locus in vivo Small Animal µCT scanner, Ohio University µCT Scanning Facility
Protosuchus haughtoni	BP/1/4770	PrHa	0.0538	Nikon Metrology XTH 225/320 LC dual source industrial CT system, University of the Witwatersrand, Johannesburg
'Steneosaurus' cf. gracilirostris	NHMUK PV OR 33095	StGr	0.089	Nikon XT H 225S CTsystem, Natural History Museum, London
Steneosaurus bollensis	BSPG 1984 I258	StBo1	0.043	Nanotom Scan, Zoologische Staatsammlung München
Steneosaurus bollensis	MCZ 1063	StBo2	0.404297	micro CT scanner at the American Museum of Natural History
Steneosaurus pictaviensis	LPP.M.35	StPi	0.140036	RX-solutions EasyTom XL Duo, Plateforme de Microtomographie, University of Poitiers
Pelagosaurus typus	NHMUK PV OR 32599	PtTy	0.098627983	Nikon XT H 225S CTsystem, Natural History Museum, London
Metriorhynchus superciliosus	MNHN.F RJN 256	MeSu1	0.10358673X 0.265	Muséum national d'Histoire naturelle, Paris, France
Metriorhynchus superciliosus	NHMUK PV R11999	MeSu2	0.12	µ-VIS X-Ray Imaging Centre, University of Southampton
Metriorhynchus superciliosus	AMNH 997	MeSu3	0.14177665	micro CT scanner at the American Museum of Natural History
Cricosaurus araucanensis	MLP 72-IV-7-1	CrAu1	0.448X0.448	SNSB X-ray facility
Cricosaurus araucanensis	MLP 76-XI-19-1	CrAu2	0.39	SNSB X-ray facility
Cricosaurus schroederi	MMGLV #	CrSc	0.5	Leibniz Institute for Zoo and Wildlife Research, Berlin
'Metriorhynchus' brachyrhynchus	NHMUK PV OR 32618	MeBr	0.0546	µ-VIS X-Ray Imaging Centre, University of Southampton
Torvoneustes coryphaeus	MJML K1863	ToCo	0.2267	µ-VIS X-Ray Imaging Centre, University of Southampton
Shamosuchus djadochtaensis	IGM 100-1195	ShDj	0.011260684	micro CT scanner at the American Museum of Natural History
Alligator mississippiensis	USNM 211232	AlMi4	0.625	Ohio Health O'Bleness Hospital
Alligator mississippiensis	USNM 211233	AlMi5	0.625	Ohio Health O'Bleness Hospital
Alligator mississippiensis	OUVC 9761	AlMi6	0.5X1	Ohio Health O'Bleness Hospital
Caiman crocodilus	FMNH 73711	CaCr	0.065X0.142	University of Texas, Austin
Crocodylus acutus	FMNH 59071	CrAc	0.625	Ohio Health O'Bleness Hospital
Crocodylus johnstoni	TMM M-6807	CrJo	0.223	University of Texas High-Resolution X-ray CT Facility
Crocodylus moreletii	TMM M-4980	CrMo	0.1904X0.5	High-Resolution X-ray CT Facility, University of Texas
Crocodylus rhombifer	MNB AB50.0171	CrRh	0.1748X0.5	High-Resolution X-ray CT Facility, University of Texas
Mecistops cataphractus	TMM M-3529	CrCa	0.165X0.5	High-Resolution X-ray CT Facility, University of Texas
Gavialis gangeticus	UF-herp-118998	GaGa2	0.14654672	Florida Museum of Natural History Herpetology
Gavialis gangeticus	TMM M-5490	GaGa1	0.228	High-Resolution X-ray CT Facility, University of Texas
Osteolaemus tetraspis	FMNH 98936	OsTe	0.0546875X0 .1108	High-Resolution X-ray CT Facility, University of Texas
Tomistoma schlegelii	TMM M-6342	ToSc1	0.165X0.46	High-Resolution X-ray CT Facility, University of Texas
Tomistoma schlegelii	USNM 211322	ToSc2	0.625	Ohio Health O'Bleness Hospital

Table S2. Information of the habitat (ecomorphology) and age of each species used in our sample.

Taxa	habitat	Age	Reason	Reference
Junggarsuchus sloani	terrestrial	M. Jurassic	Inferred, from deposit, and limb-dimensions and cranial shape	1
Undescribed sphenosuchian	terrestrial	Carnian	Inferred, from deposit, and limb-dimensions and cranial shape	NCSM 21722
Eopneumatosuchus colberti	semiaquatic	Sinemurian*	Inferred, from deposit and cranial shape	2
Protosuchus haughtoni	terrestrial	Hettangian	Inferred, from post-cranial skeleton	3
'Steneosaurus' gracilirostris	semiaquatic	Toarcian	Inferred, from a marine deposit, but has extant-like limbs, and has osteoderms	4
Steneosaurus bollensis	semiaquatic	Toarcian	Inferred, from a marine deposit, but has extant-like limbs, and has osteoderms	4
Steneosaurus pictaviensis	semiaquatic	Toarcian	Inferred, from a marine deposit and is a teleosaurid	5
Pelagosaurus typus	semiaquatic	Toarcian	Inferred, from a marine deposit, but has extant-like limbs, and has osteoderms	4
Metriorhynchus superciliosus	pelagic	Callovian	Inferred, marine deposit, has flippers and a tail-fin	5
Cricosaurus araucanensis	pelagic	Tithonian	Inferred, marine deposit, has flippers and a tail-fin	6, 7
Cricosaurus schroederi	pelagic	Valanginian	Inferred, marine deposit and is a metriorhynchid	8
'Metriorhynchus' brachyrhynchus	pelagic	Callovian	Inferred, marine deposit and has a tail-fin	5
Torvoneustes coryphaeus	pelagic	Kimmeridgian	Inferred, marine deposit and is a metriorhynchid	9
Shamosuchus djadochtaensis	semiaquatic	L. Cretaceous	Inferred, based on post-cranial anatomy	10
Alligator mississippiensis	semiaquatic	Recent	extant, observed	e.g. 11
Caiman crocodilus	semiaquatic	Recent	extant, observed	e.g. 11
Crocodylus acutus	semiaquatic	Recent	extant, observed	e.g. 11
Crocodylus johnstoni	semiaquatic	Recent	extant, observed	e.g. 11
Crocodylus moreletii	semiaquatic	Recent	extant, observed	e.g. 11
Crocodylus rhombifer	semiaquatic	Recent	extant, observed	e.g. 11
Mecistops cataphractus	semiaquatic	Recent	extant, observed	e.g. 11
Gavialis gangeticus	semiaquatic	Recent	extant, observed	e.g. 11
Osteolaemus tetraspis	semiaquatic	Recent	extant, observed	e.g. 11
Tomistoma schlegelii	semiaquatic	Recent	extant, observed	e.g. 11

*The age of the Kayenta Formation may be Pliensbachian-Toarcian, as has been presented in a conference abstract (Marsh et al., 2014, Society of Vertebrate Paleontology Annual Meeting).

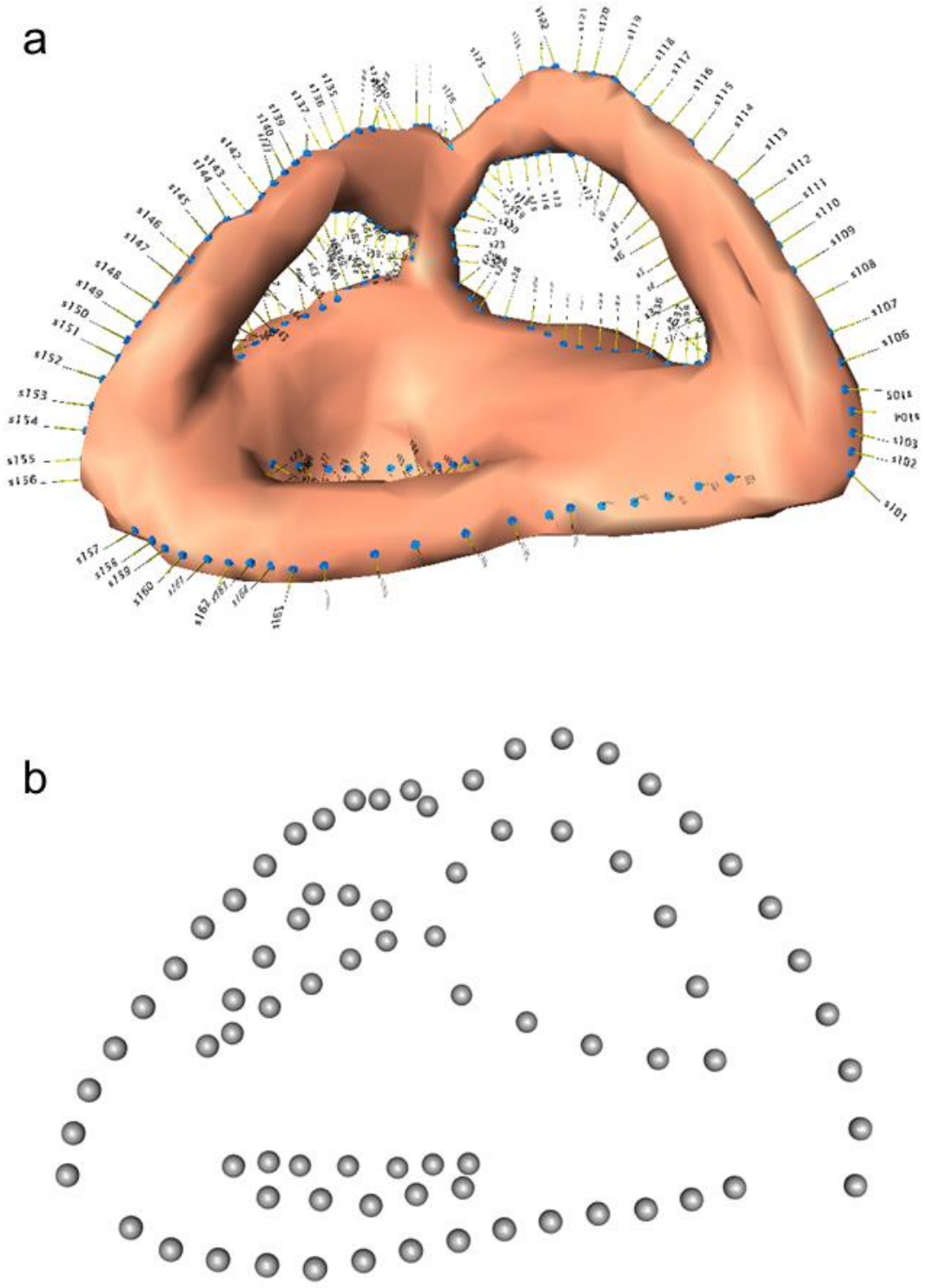

Fig. S1. Landmark placing on the right labyrinth of *Metriorhynchus supercilious* (NHMUK PV R11999). a, landmark placement in the IDAV Landmark software; b, evenly spaced semilandmarks on the three semicircular canals, 11 on the internal surface and 12 on the external surface (see methods section for details).

3. Principal component analysis

Table S3. Results of the Principal Component Analysis. PCA coordinates for the first 31 PC axes.

	PC1	PC2	PC3	PC4	PC5	PC6	PC7	PC8
AlMi4	-0.025	-0.024	0.035	-0.038	0.013	-0.002	0.009	0.000
AlMi5	-0.022	-0.050	0.025	-0.044	0.000	-0.007	0.010	-0.003
CaCr	-0.051	-0.043	-0.011	-0.037	-0.025	-0.001	0.010	0.028
CrAc	-0.016	-0.056	0.015	0.025	0.022	-0.030	-0.020	-0.006
CrMo	-0.061	-0.021	-0.019	0.013	0.011	0.012	-0.014	-0.004
CrJo	-0.059	-0.003	-0.004	-0.059	0.012	0.000	0.012	-0.028
CrCa	-0.014	-0.085	0.022	0.047	0.011	-0.023	0.005	-0.004
OsTe	-0.030	-0.002	0.049	-0.003	-0.035	-0.044	-0.012	0.034
GaGa1	-0.028	-0.056	0.054	-0.006	0.004	-0.008	0.005	0.004
ToSc1	-0.051	-0.069	0.013	0.027	0.013	0.014	-0.007	0.014
ToSc2	-0.022	-0.071	0.035	0.025	0.009	0.027	-0.017	0.021
GaGa2	-0.032	-0.010	0.058	-0.023	0.037	0.028	-0.019	0.005
AlMi6	-0.038	0.013	0.028	-0.045	0.001	-0.011	0.042	-0.030
CrRh	-0.033	-0.053	0.002	0.039	0.001	0.036	0.001	-0.005
PeTy	0.014	0.084	0.028	0.006	-0.043	0.010	-0.016	-0.002
JuSl	-0.115	0.019	-0.064	0.031	-0.033	-0.056	0.012	0.002
MeSu2	0.057	0.015	-0.016	-0.041	0.038	0.003	0.048	0.032
StBo1	0.011	0.056	0.058	0.023	-0.011	0.013	-0.017	0.013
CrSc	0.104	-0.092	-0.062	-0.005	-0.077	0.060	-0.011	-0.047
EoCo	-0.048	0.066	-0.030	0.009	0.014	0.046	-0.020	-0.021
UnSp	-0.087	0.039	-0.065	-0.008	-0.081	-0.015	0.016	0.012
MeSu1	0.038	0.064	-0.037	-0.004	0.001	0.031	0.031	0.033
StBo2	0.014	0.097	0.059	0.018	-0.012	-0.024	0.006	-0.056
StGr	0.059	0.066	0.029	0.051	-0.018	0.001	0.005	0.001
MeBr	0.072	0.063	-0.009	0.000	0.040	-0.006	0.049	0.005
MeSu3	0.028	0.039	-0.022	0.005	-0.004	0.041	0.029	0.031
CrAu1	0.136	0.008	0.021	-0.074	-0.026	-0.023	-0.073	0.037
PrHa	-0.071	0.101	-0.096	-0.005	0.060	-0.002	-0.071	-0.005
ToCo	0.115	-0.065	-0.110	0.057	0.025	-0.042	0.005	0.017
CrAu2	0.087	-0.028	-0.032	-0.047	0.019	-0.044	-0.003	-0.052
StPi	0.073	0.031	0.068	0.069	0.005	-0.011	0.002	-0.013
ShDj	-0.003	-0.035	-0.025	-0.007	0.027	0.025	0.002	-0.016

	PC9	PC10	PC11	PC12	PC13	PC14	PC15	PC16
AlMi4	0.028	-0.006	-0.019	0.014	-0.035	-0.013	-0.002	0.039
AlMi5	0.016	-0.002	0.026	-0.018	-0.009	-0.018	0.008	0.008
CaCr	0.008	-0.005	-0.012	-0.020	0.014	0.003	-0.024	0.008
CrAc	0.042	-0.010	0.014	-0.023	0.040	0.005	0.015	0.002
CrMo	-0.023	-0.018	-0.003	-0.014	0.011	0.015	0.006	0.005
CrJo	-0.030	-0.022	-0.008	0.022	-0.004	0.008	0.026	-0.013
CrCa	-0.032	-0.010	0.024	0.005	0.012	-0.010	0.023	0.001
OsTe	0.012	-0.040	0.003	-0.001	-0.022	0.034	-0.015	-0.012
GaGa1	0.014	0.018	0.010	0.004	-0.002	0.007	-0.001	0.006
ToSc1	-0.013	0.017	0.005	0.006	0.010	-0.017	-0.003	-0.005
ToSc2	0.032	0.013	0.006	0.024	-0.020	-0.036	-0.005	-0.026
GaGa2	0.008	0.028	-0.012	-0.011	0.014	0.026	-0.015	-0.013
AlMi6	-0.002	-0.034	-0.017	-0.022	0.009	-0.024	-0.022	-0.017
CrRh	-0.025	-0.015	-0.004	0.017	-0.006	0.018	0.004	0.024
PeTy	-0.017	-0.014	0.002	-0.011	0.007	-0.022	-0.013	0.015
JuSl	0.005	0.045	-0.053	-0.014	-0.010	-0.003	0.027	-0.004
MeSu2	-0.023	0.009	0.024	-0.006	-0.015	0.008	0.026	0.009
StBo1	-0.016	0.021	0.007	-0.017	-0.030	0.015	0.001	-0.004
CrSc	0.036	-0.009	-0.008	-0.010	-0.006	0.013	0.018	-0.003
EoCo	-0.007	0.001	0.004	-0.006	-0.030	-0.008	-0.005	-0.015
UnSp	-0.007	0.005	0.041	0.044	0.013	0.003	-0.012	-0.005
MeSu1	0.028	0.012	-0.013	0.012	0.026	-0.010	-0.006	0.017
StBo2	0.006	0.012	0.013	-0.009	-0.002	0.012	-0.003	0.008
StGr	-0.022	-0.011	0.002	-0.022	0.005	-0.032	0.012	-0.002
MeBr	0.033	-0.024	-0.013	0.022	0.002	0.006	0.016	-0.021
MeSu3	-0.001	0.020	0.018	-0.025	0.011	0.017	0.000	-0.007
CrAu1	-0.025	0.002	-0.021	0.011	0.012	-0.008	0.017	-0.005
PrHa	0.027	-0.018	0.015	0.004	0.003	-0.002	0.003	0.008
ToCo	-0.010	-0.016	-0.002	-0.015	-0.025	0.001	-0.028	-0.001
CrAu2	-0.005	0.045	0.023	0.009	0.000	-0.001	-0.020	0.000
StPi	0.011	0.001	-0.020	0.040	0.012	0.011	-0.006	0.005
ShDj	-0.048	0.004	-0.031	0.011	0.016	0.002	-0.023	0.000

	PC17	PC18	PC19	PC20	PC21	PC22	PC23	PC24
AlMi4	-0.013	0.000	-0.005	-0.001	-0.005	0.018	0.002	0.002
AlMi5	-0.012	0.000	0.018	0.009	-0.003	-0.006	-0.015	-0.015
CaCr	-0.011	-0.008	0.008	0.001	0.033	-0.004	0.002	0.011
CrAc	-0.007	0.007	0.006	-0.007	-0.002	0.007	-0.009	0.013
CrMo	-0.011	0.010	0.004	-0.004	0.004	0.001	0.009	-0.019
CrJo	-0.004	-0.002	0.016	0.011	0.001	-0.011	0.011	0.017
CrCa	0.012	-0.011	-0.003	-0.002	0.003	0.015	0.011	0.000
OsTe	0.027	0.014	-0.008	-0.008	-0.002	-0.001	-0.005	0.001
GaGa1	0.012	-0.003	0.002	0.004	-0.002	-0.015	-0.002	-0.009
ToSc1	-0.007	0.001	-0.023	-0.023	0.005	-0.008	0.000	0.002
ToSc2	-0.001	0.006	0.004	0.004	-0.008	-0.009	0.005	0.007
GaGa2	0.005	-0.029	-0.014	0.022	-0.003	0.005	0.003	-0.006
AlMi6	0.008	0.003	-0.004	-0.003	-0.014	0.012	0.010	-0.004
CrRh	0.014	0.004	0.011	0.001	-0.003	-0.013	0.000	-0.007
PeTy	0.006	0.002	-0.009	0.013	-0.002	-0.014	-0.006	0.010
JuSl	0.007	0.002	0.000	0.004	-0.004	-0.001	-0.004	-0.001
MeSu2	0.011	-0.007	-0.020	-0.001	0.000	0.003	-0.009	0.010
StBo1	-0.026	0.021	-0.006	0.000	0.006	0.006	0.016	0.002
CrSc	0.002	-0.001	-0.015	0.002	0.000	0.002	0.001	0.001
EoCo	0.017	-0.015	0.019	-0.018	0.015	0.013	-0.013	-0.001
UnSp	-0.015	-0.009	-0.005	0.005	-0.004	0.010	-0.003	-0.005
MeSu1	0.021	0.000	0.007	-0.012	-0.002	-0.003	0.017	-0.003
StBo2	-0.012	-0.021	0.001	-0.021	-0.010	-0.015	0.003	0.003
StGr	0.006	0.002	-0.006	0.016	0.011	0.001	-0.003	-0.007
MeBr	-0.017	0.004	-0.009	-0.003	0.013	-0.010	-0.005	-0.012
MeSu3	-0.004	0.014	0.022	0.002	-0.017	0.006	-0.002	0.006
CrAu1	-0.004	-0.009	0.009	-0.011	-0.006	0.002	0.000	-0.006
PrHa	0.002	0.006	-0.011	0.009	-0.003	-0.002	0.003	0.001
ToCo	-0.011	-0.018	0.007	0.005	-0.008	-0.005	0.005	0.002
CrAu2	0.017	0.023	0.001	0.003	0.013	0.001	0.005	-0.003
StPi	0.000	0.001	0.013	0.011	0.005	0.014	-0.007	0.006
ShDj	-0.011	0.014	-0.009	-0.005	-0.010	0.000	-0.019	0.003

	PC25	PC26	PC27	PC28	PC29	PC30	PC31
AlMi4	-0.001	-0.002	-0.014	0.005	0.000	0.002	0.001
AlMi5	0.001	-0.003	0.010	-0.007	0.001	-0.010	0.008
CaCr	0.010	-0.001	0.002	0.001	-0.004	-0.003	-0.006
CrAc	-0.010	-0.004	0.000	0.001	0.010	0.008	-0.001
CrMo	-0.015	-0.005	-0.005	-0.008	-0.015	0.005	-0.002
CrJo	-0.004	-0.004	-0.002	0.005	0.000	0.002	0.008
CrCa	0.018	0.006	-0.007	-0.010	0.002	-0.004	0.001
OsTe	0.002	-0.008	-0.004	-0.001	-0.001	-0.004	0.005
GaGa1	0.010	0.015	0.003	0.007	-0.006	0.018	0.003
ToSc1	-0.010	0.007	-0.001	0.011	-0.003	-0.010	0.008
ToSc2	0.000	-0.010	-0.001	-0.007	-0.004	0.001	-0.009
GaGa2	-0.005	-0.005	-0.005	-0.001	0.005	-0.003	0.001
AlMi6	-0.002	0.009	0.011	0.004	0.000	-0.001	-0.005
CrRh	-0.004	0.000	0.004	0.006	0.013	-0.006	-0.011
PeTy	-0.010	0.015	-0.009	-0.012	0.002	0.001	0.001
JuSl	0.000	0.002	0.001	-0.002	0.001	-0.002	-0.002
MeSu2	-0.007	-0.003	0.010	-0.003	-0.006	0.002	-0.006
StBo1	0.002	0.004	0.012	-0.003	0.009	0.004	0.003
CrSc	0.003	0.001	0.003	0.000	-0.003	-0.001	0.002
EoCo	-0.004	0.004	-0.002	-0.001	0.003	0.005	0.002
UnSp	-0.003	-0.002	0.001	0.002	0.003	0.004	-0.001
MeSu1	0.000	-0.009	0.005	-0.006	0.004	0.002	0.008
StBo2	0.006	-0.009	-0.001	-0.001	-0.004	-0.002	-0.004
StGr	0.004	-0.017	-0.003	0.014	-0.001	0.003	0.001
MeBr	0.003	0.008	-0.009	-0.003	0.007	-0.001	-0.003
MeSu3	0.006	0.007	-0.013	0.007	-0.006	-0.006	-0.001
CrAu1	0.000	0.003	0.001	0.002	0.001	0.000	-0.004
PrHa	0.011	0.003	0.006	0.003	-0.004	-0.004	-0.001
ToCo	-0.005	0.002	0.001	0.001	0.001	0.002	0.003
CrAu2	-0.005	-0.002	-0.006	0.000	0.002	-0.003	-0.002
StPi	-0.005	0.006	0.011	0.000	-0.011	-0.005	0.002
ShDj	0.014	-0.009	0.001	-0.006	0.002	0.005	0.003

Table S4. Results of the Principal Component Analysis. Variance (%) and Cumulative Proportion (%) for the first 31 principal component axes.

	Variance (%)	Cumulative Proportion (%)
PC1	22.269	22.269
PC2	18.443	40.713
PC3	12.386	53.099
PC4	7.336	60.435
PC5	5.641	66.076
PC6	4.605	70.681
PC7	4.183	74.864
PC8	3.487	78.351
PC9	3.100	81.450
PC10	2.368	83.819
PC11	2.124	85.943
PC12	1.951	87.894
PC13	1.702	89.596
PC14	1.525	91.121
PC15	1.454	92.575
PC16	1.006	93.581
PC17	0.918	94.498
PC18	0.769	95.267
PC19	0.748	96.015
PC20	0.597	96.612
PC21	0.540	97.152
PC22	0.483	97.635
PC23	0.409	98.044
PC24	0.374	98.418
PC25	0.325	98.743
PC26	0.309	99.053
PC27	0.262	99.315
PC28	0.197	99.511
PC29	0.196	99.707
PC30	0.167	99.874
PC31	0.126	100.000

4. Morphospace clustering analysis

Table S5. Results of the PERMANOVA, to test if the three habitat groups are statistically significantly different form each other.

pairs	F Model	R2	p value	p adjusted
semiaquatic vs. terrestrial	4.875	0.223	0.002	0.003
semiaquatic vs. pelagic	5.302	0.218	0.002	0.003
terrestrial vs. pelagic	4.543	0.431	0.012	0.012

5. Canonical variate analysis

Table S6. Results for the canonical variate analysis (CVA). Showing the classification of the three habitat groups (pelagic, semiaquatic, terrestrial) with an overall classification accuracy of 100%.

	pelagic	semiaquatic	terrestrial
pelagic	100	0	0
semiaquatic	0	100	0
terrestrial	0	0	100

overall classification accuracy: 100 %

	CV 1	CV 2
AlMi4	-1.033	0.846
AlMi5	-0.485	1.594
CaCr	-0.128	-0.364
CrAc	-2.027	0.536
CrMo	-3.402	0.029
CrJo	-2.502	-0.035
CrCa	-3.322	1.787
OsTe	-3.384	-0.204
GaGa1	-2.031	1.215
ToSc1	-2.747	0.397
ToSc2	-1.644	0.679
GaGa2	-2.243	2.108
AlMi6	-2.406	2.322
CrRh	-3.277	1.411
PeTy	-1.567	0.197
JuSl	-1.680	-7.193
MeSu2	5.803	1.926
StBo1	-1.803	1.280
CrSc	5.133	1.732
EoCo	-1.782	-1.412
UnSp	0.071	-7.272
MeSu1	5.550	-1.380
StBo2	-2.583	0.189
StGr	-0.300	2.021
MeBr	4.587	0.826
MeSu3	4.047	0.695
CrAu1	4.832	0.948
PrHa	-0.600	-6.291
ToCo	6.925	-0.480
CrAu2	5.415	-0.885
StPi	-1.109	1.514
ShDj	-0.307	1.266

6. Phylogenies used for phylogenetic comparative methods

The main phylogenetic framework used herein is based on the results from Young *et al*. (12). This dataset (the 'H+Y dataset') is the latest in the ongoing Crocodylomorph SuperMatrix Project, a continuously updated dataset investigating the evolutionary relationships of crocodylomorph archosaurs. It was first presented in Ristevski *et al*. (13), and has been subsequently updated (e.g. 14–17). It is one of three datasets that form the core of the Crocodylomorph SuperMatrix Project, the other two also being presented in a modified form in Ősi *et al*. (14).

However, there are some taxa we use in our datasets that are known to have differing positions phylogenetically. The first of which is *Eopneumatosuchus colberti*. It has been recovered as the basal-most thalattosuchian in the 'H+Y dataset'. However, in Young *et al*. (12), the position of *Eopneumatosuchus* can change depending on use of implied weighting or using Bayesian methods. In those analyses, *Eopneumatosuchus* is recovered as the sister taxon to Shartegosuchoidea + Mesoeucrocodylia. To test whether this second possible position of *Eopneumatosuchus* alters our result, we ran a series of sensitivity analyses with *Eopneumatosuchus* placed as the sister taxon to Thalattosuchia + (*Shamosuchus* + Crocodylia).

The second species we ran sensitivity analyses on was *Pelagosaurus typus*. While the more recent and large-sampled thalattosuchians phylogenetic datasets recover *Pelagosaurus* as the basal-most member of Metriorhynchoidea (papers using the 'H+Y' dataset, 18), some earlier datasets and pre-phylogenetic opinions considered *Pelagosaurus* to be a teleosauroid (e.g. 4, 19; although see Buffetaut (20) for a metriorhynchid-like opinion). We tested this alternate position of *Pelagosaurus* to see if it impacted upon our results.

There are also some competing hypotheses for the relationships of extant crocodylians in our dataset. In particular, there is no consensus on whether *Osteolaemus tetraspis* is more closely related to *Mecistops* or *Crocodylus*, in either molecular or morphological phylogenies (21). Additionally, the position of *Gavialis gangeticus* differs between molecular and morphological datasets. Molecular datasets recover *Gavialis* as the sister taxon to *Tomistoma* (being within Crocodylidae) – a position the Young *et al*. (12) dataset also recovers (e.g. 21, 22). However, most morphology-only datasets recover *Gavialis* as the basal-most living species, being the sister taxon to Alligatoridae + Crocodylidae (for further analyses and discussion see 23). However, as these both concern small nuances of the relationships of extant crocodylians—all of which have semiaquatic-type ears—these rearrangements would not affect our results.

7. Pagel's Lambda analysis

Table S7. Results for the phylogenetic influence tested with the Pagel's lambda tested for three different phylogenies: our primary phylogeny (first listed) and two alternative trees, for sensitivity analysis (see Section 6 above). 0 → no correlation between species; 1 → correlation between species equal to the Brownian expectation/the structure of the phylogeny alone can explain changes in traits.

Primary phylogeny

	lambda	logL	logL0	p value
PC1	0.99996	28.705	16.435	0.00000073
PC2	0.69646	31.134	22.893	0.00004913
PC3	0.99993	31.597	18.921	0.00000048

***Eopneumatosuchus colberti* placed as the sister taxon to Thalattosuchia + (*Shamosuchus* + Crocodylia)**

	lambda	logL	logL0	p value
PC1	0.77400	27.769	16.506	2E-06
PC2	0.65831	30.953	22.949	6E-05
PC3	0.99993	32.243	19.051	3E-07

***Pelagosaurus typus* positioned as a teleosauroid**

	lambda	logL	logL0	p value
PC1	0.77400	27.769	16.506	2E-06
PC2	0.65831	30.953	22.949	6E-05
PC3	0.99993	32.243	19.051	3E-07

8. pGLS regressions

Table S8. Results for Ordinary least squares (OLS) and phylogenetic generalised least squares (pGLS), using our primary phylogeny. First correlating the raw PC scores and centroid size (labyrinth size); second, correlating the raw PC scores and habitat; third correlating the residuals from the PC scores and centroid size with habitat.

Primary phylogeny

Model	Type	AICc	intercept	p value	slope	p value	R2
PC1~centroid size	OLS	-61.319	-4.706	0.111	4.662	0.112	0.071
	pGLS	-78.643	-5.078	0.034	4.993	0.035	0.111
PC2~centroid size	OLS	-64.049	-0.531	0.845	0.527	0.845	-0.044
	pGLS	-76.99	8.307	0.002	-8.208	0.002	0.418
PC3~centroid size	OLS	-88.324	7.205	0.0002	-7.149	0.0002	0.451
	pGLS	-81.948	5.787	0.011	-5.751	0.011	0.315
PC1~pelagic	OLS	-78.162	-0.028	0.012	0.116	2.65e-05	0.559
	pGLS	-70.159	-0.035	0.370	0.083	0.042	0.385
PC2~pelagic	OLS	-64.329	0.0033	0.81	-0.016	0.59	0.013
	pGLS	-60.347	0.002	0.974	-0.060	0.222	-0.165
PC3~pelagic	OLS	-76.934	0.0035	0.734	-0.046	0.056	0.156
	pGLS	-68.628	-0.031	0.445	-0.050	0.226	-0.193
PC1.residuals~pelagic	OLS	-72.660	-0.019	0.110	0.089	0.00143	0.377
	pGLS	-59.892	0.018	0.703	0.089	0.0005	-0.061
PC2.residuals~pelagic	OLS	-64.505	0.004	0.769	-0.019	0.522	0.019
	pGLS	-49.136	-0.038	0.522	0.007	0.801	-0.861
PC3.residuals~pelagic	OLS	-88.418	0.001	0.895	-0.005	0.773	0.004
	pGLS	-68.295	0.003	0.940	0.008	0.847	-1.304

Table S9. Results for phylogenetic generalised least squares (pGLS), using the two alternative phylogenies. First correlating the raw PC scores and centroid size (labyrinth size); second, correlating the raw PC scores and habitat; third correlating the residuals from the PC scores and centroid size with habitat.

***Eopneumatosuchus colberti* placed as the sister taxon to Thalattosuchia + (*Shamosuchus* + Crocodylia)**

Model	Type	AICc	intercept	p value	slope	p value	R2
PC1~centroid size	pGLS	-76.721	-4.918	0.069	4.838	0.069	0.532
PC2~centroid size	pGLS	-77.183	7.885	0.005	-7.790	0.005	0.422
PC3~centroid size	pGLS	-83.430	5.577	0.019	-5.544	0.019	0.356
PC1~pelagic	pGLS	-70.159	-0.035	0.370	0.083	0.042	0.385
PC2~pelagic	pGLS	-60.347	0.002	0.974	-0.060	0.222	-0.165
PC3~pelagic	pGLS	-68.628	-0.031	0.445	-0.049	0.226	-0.192
PC1.residuals~pelagic	pGLS	-55.657	0.009	0.859	0.092	0.001	-0.266
PC2.residuals~pelagic	pGLS	-47.624	-0.032	0.594	0.013	0.666	-0.983
PC3.residuals~pelagic	pGLS	-70.355	0.003	0.939	0.011	0.544	-1.114

***Pelagosaurus typus* positioned as a teleosauroid**

Model	Type	AICc	intercept	p value	slope	p value	R2
PC1~centroid size	pGLS	-80.371	-5.328	0.023	5.230	0.024	0.598
PC2~centroid size	pGLS	-77.218	8.343	0.002	-8.242	0.002	0.423
PC3~centroid size	pGLS	-82.687	5.655	0.012	-5.627	0.012	0.336
PC1~pelagic	pGLS	-71.177	-0.042	0.279	0.078	0.041	0.410
PC2~pelagic	pGLS	-60.562	0.0002	0.997	-0.059	0.214	-0.154
PC3~pelagic	pGLS	-69.841	-0.038	0.345	-0.052	0.174	-0.134
PC1.residuals~pelagic	pGLS	-55.436	0.008	0.887	0.089	0.001	-0.278
PC2.residuals~pelagic	pGLS	-48.265	-0.039	0.536	0.007	0.809	-0.930
PC3.residuals~pelagic	pGLS	-70.095	0.004	0.916	0.005	0.782	-1.137

9. Labyrinth character optimization on phylogeny

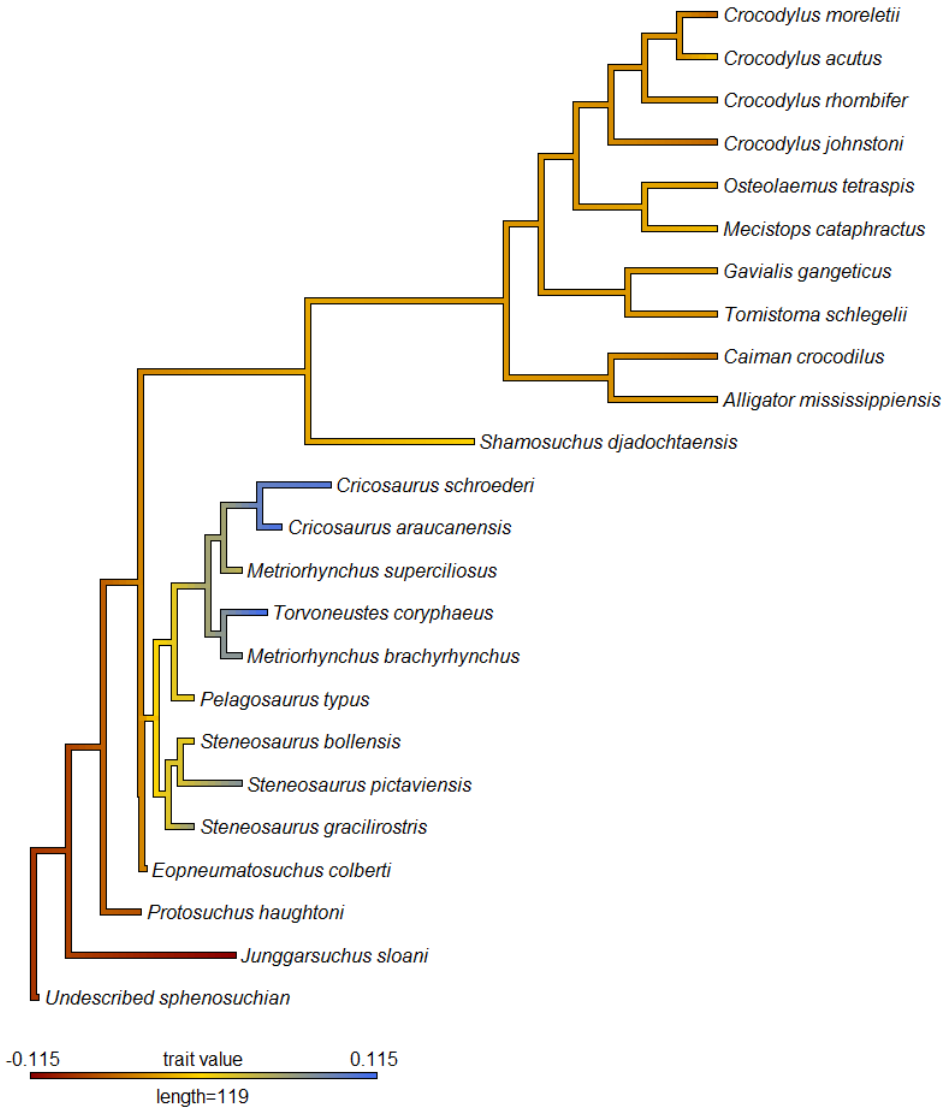

Fig. S2. PC1 scores optimized on our primary phylogeny to predict ancestral states for the major clades and assess evolutionary trends.

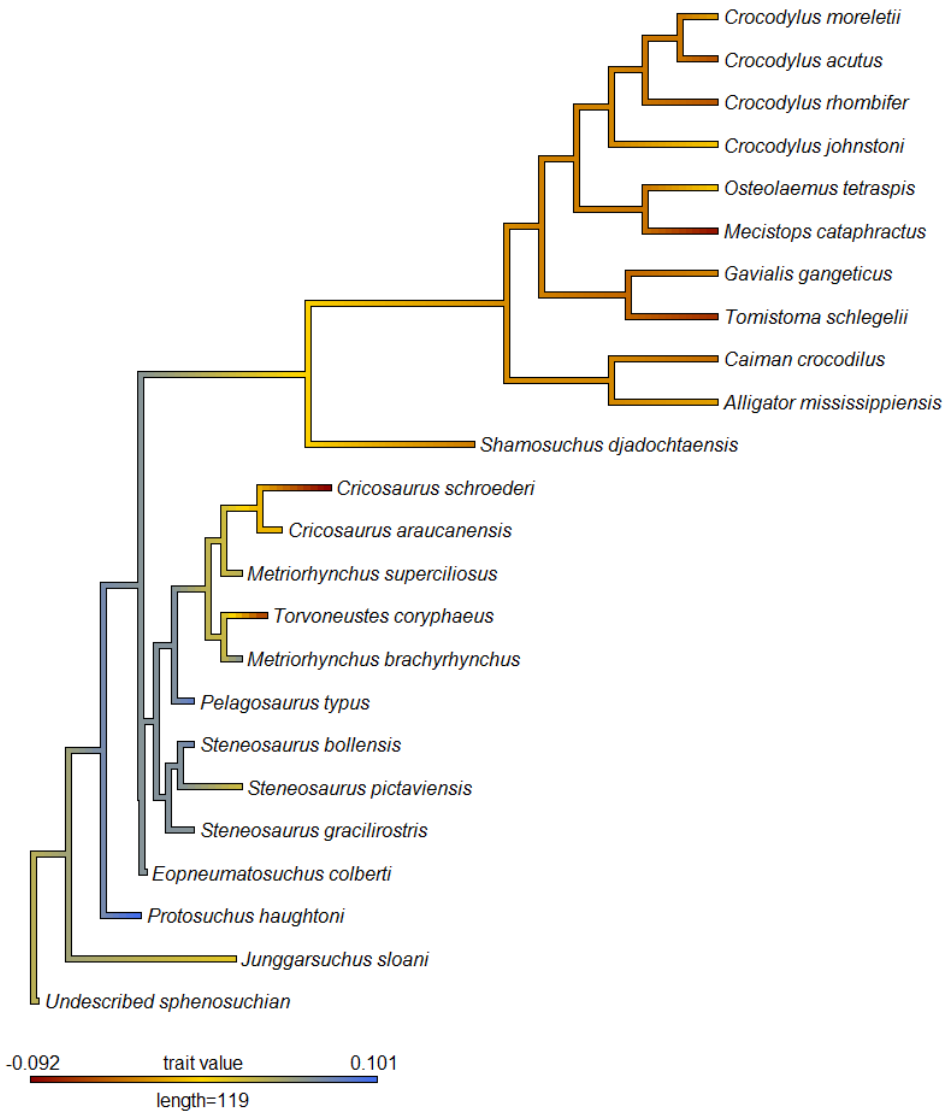

Fig. S3. PC2 scores optimized on our primary phylogeny to predict ancestral states for the major clades and assess evolutionary trends.

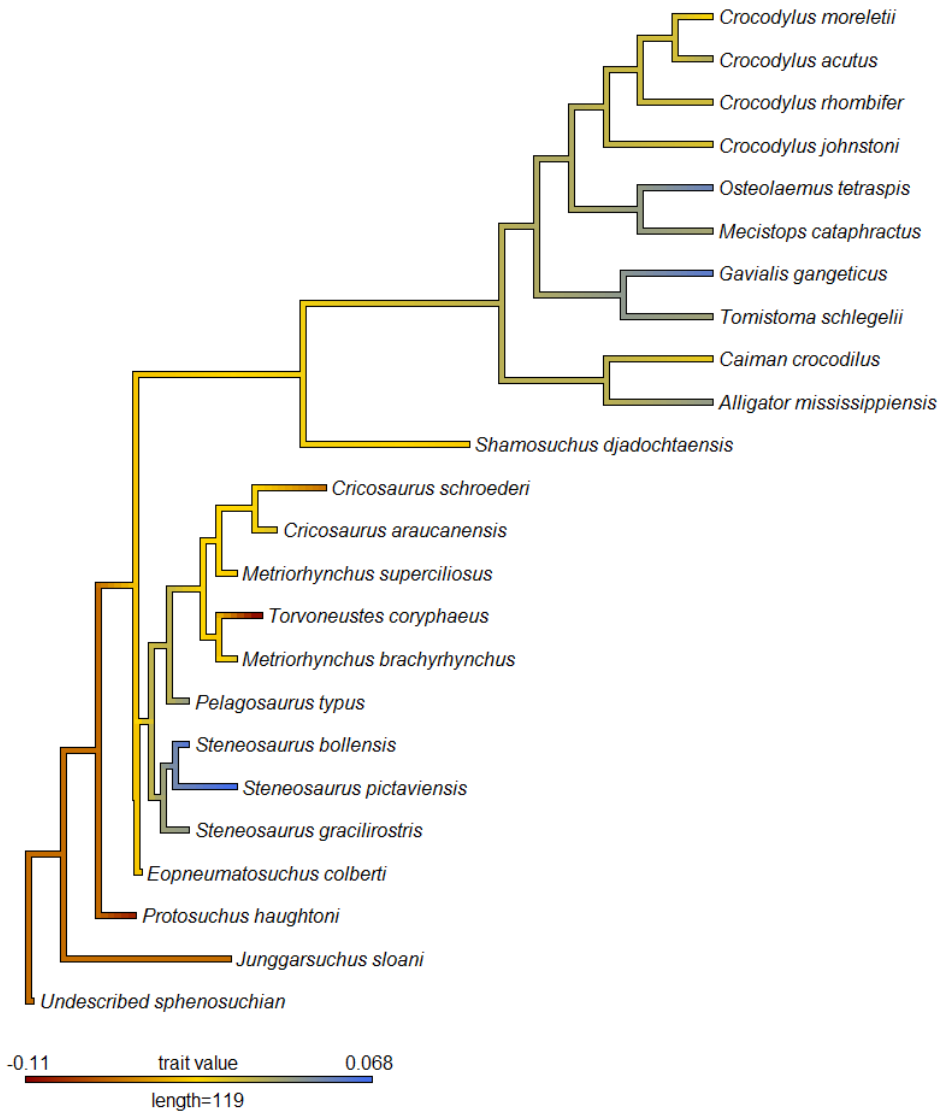

Fig. S4. PC3 scores optimized on our primary phylogeny to predict ancestral states for the major clades and assess evolutionary trends.

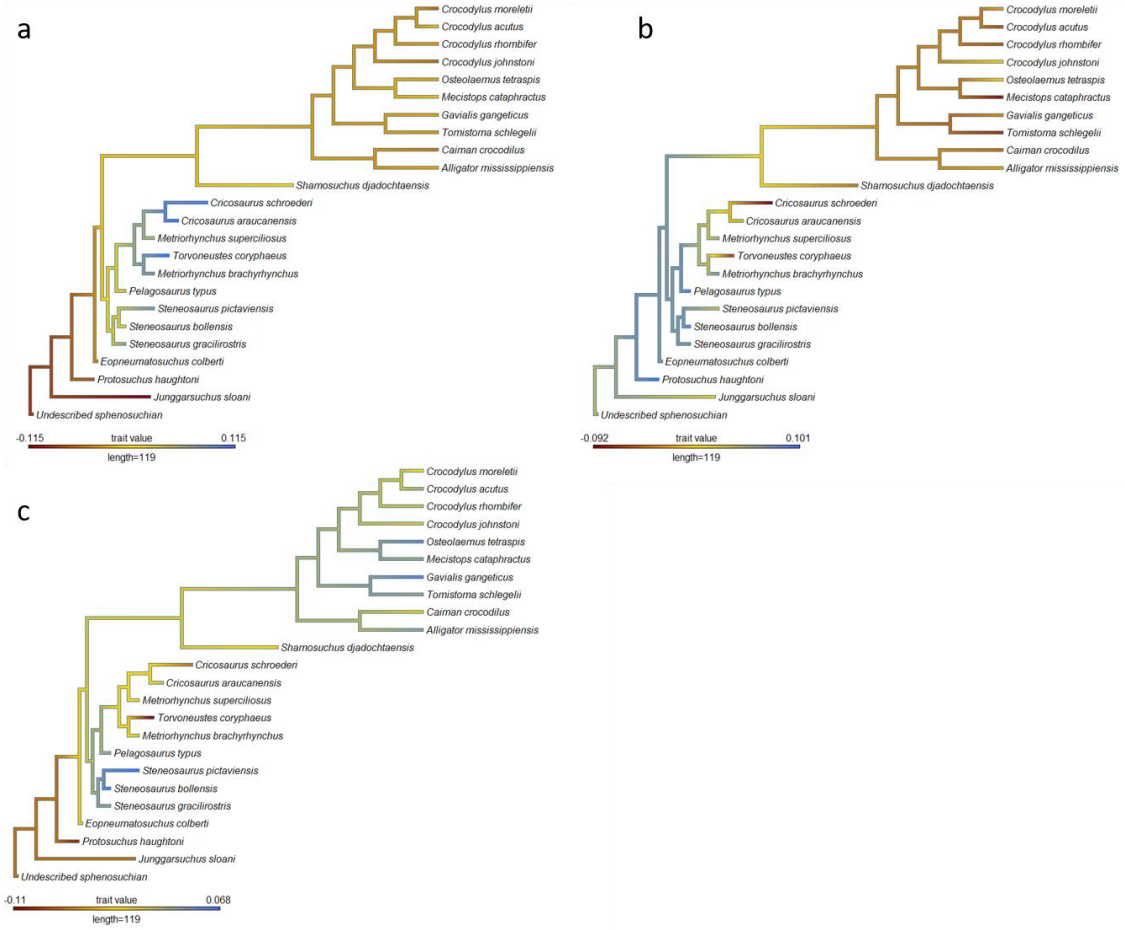

Fig. S5. PC scores of the first three principal components, optimized on the phylogeny with *Eopneumatosuchus colberti* placed as the sister taxon to Thalattosuchia + (*Shamosuchus* + Crocodylia), to predict ancestral states for the major clades and assess evolutionary trends. a, PC1; b, PC2; c, PC3.

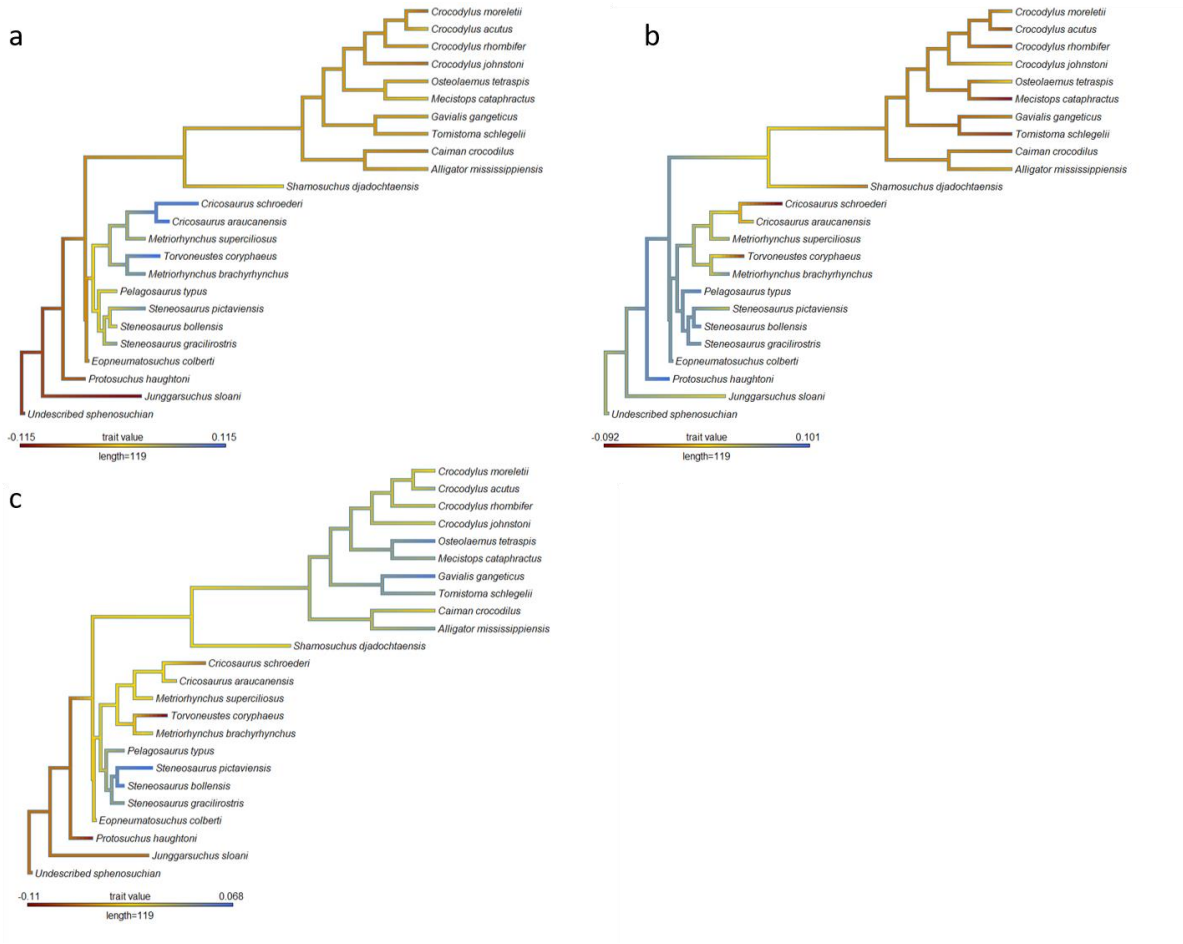

Fig. S6. PC3 scores optimized on the phylogeny with *Pelagosaurus typus* positioned as a teleosauroid, to predict ancestral states for the major clades and assess evolutionary trends. a, PC1; b, PC2; c, PC3.

10. Evolutionary model fitting

Table S10. Five standard models fitted on the first three principal component axes showing the AIC scores. The models are: BM (Brownian motion), OU (Ornstein-Uhlenbeck), EB (Early-burst), trend (Brownian motion with trend) and lambda (Pagel).

Primary phylogeny

	BM	OU	EB	trend	lambda
PC1	-74.485	-71.856	-79.996	-63.232	-71.856
PC2	-69.521	-68.680	-69.084	-64.574	-67.822
PC3	-74.591	-73.483	-78.519	-64.725	-71.962

Primary phylogeny (fossil specimens only)

	BM	OU	EB	trend	lambda
PC1	-36.607	-33.298	-33.297	-39.191	-33.305
PC2	-35.977	-34.494	-32.667	-38.418	-33.666
PC3	-42.606	-40.841	-39.524	-36.884	-39.297

***Eopneumatosuchus colberti* placed as the sister taxon to Thalattosuchia + (*Shamosuchus* + Crocodylia)**

	BM	OU	EB	trend	lambda
PC1	-72.911	-70.283	-78.911	-61.215	-70.283
PC2	-72.719	-71.107	-71.698	-67.207	-70.091
PC3	-78.059	-76.365	-80.978	-67.787	-75.429

***Pelagosaurus typus* positioned as a teleosauroid**

	BM	OU	EB	trend	lambda
PC1	-76.211	-73.582	-81.262	-65.216	-73.582
PC2	-69.629	-68.789	-69.289	-64.601	-67.825
PC3	-75.373	-74.759	-79.190	-65.683	-72.745

11. Evolutionary rates

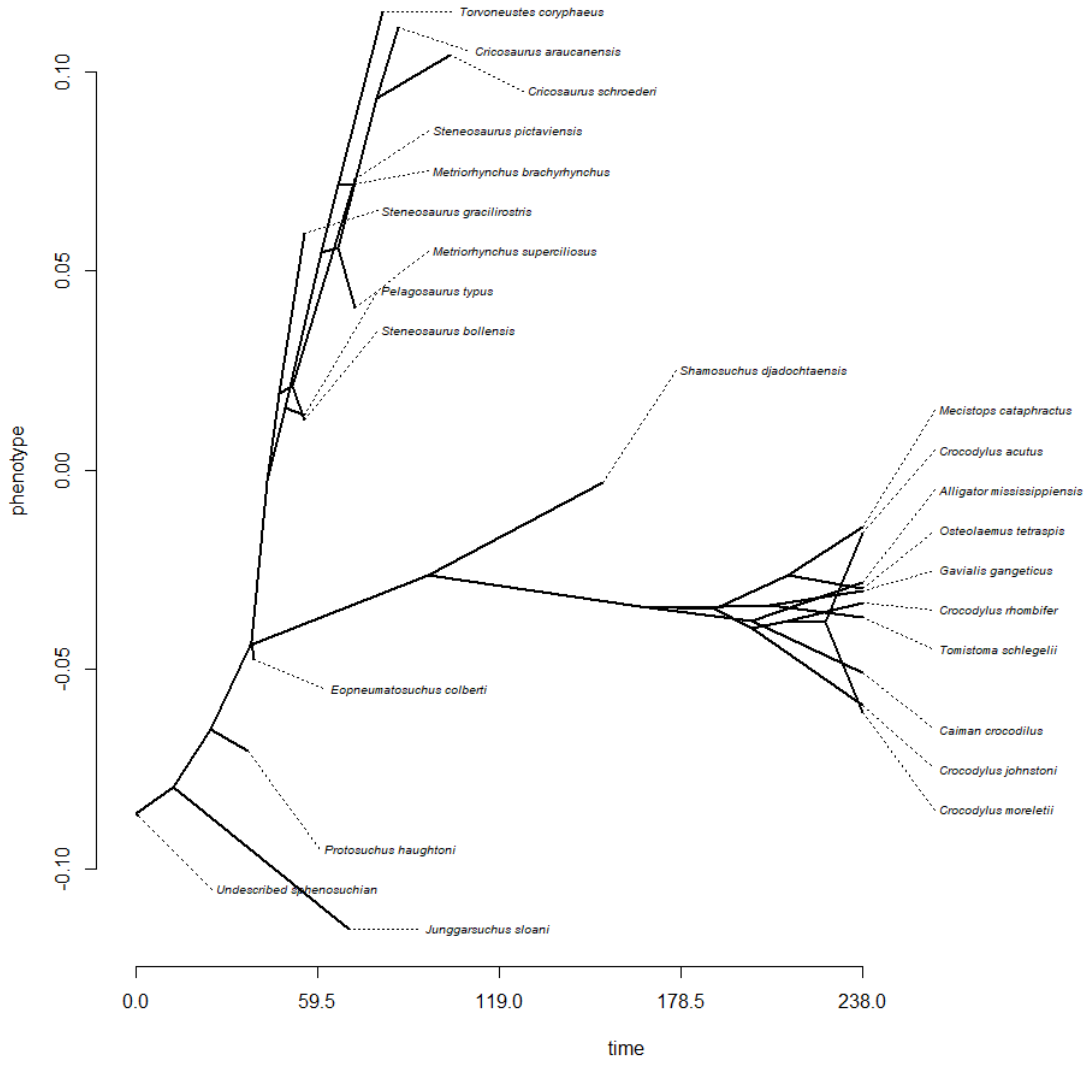

Fig. S7. The primary phylogeny is plotted such that the x-axis is scaled to time and the y-axis to PC1 score.

12. Cochlear measurements

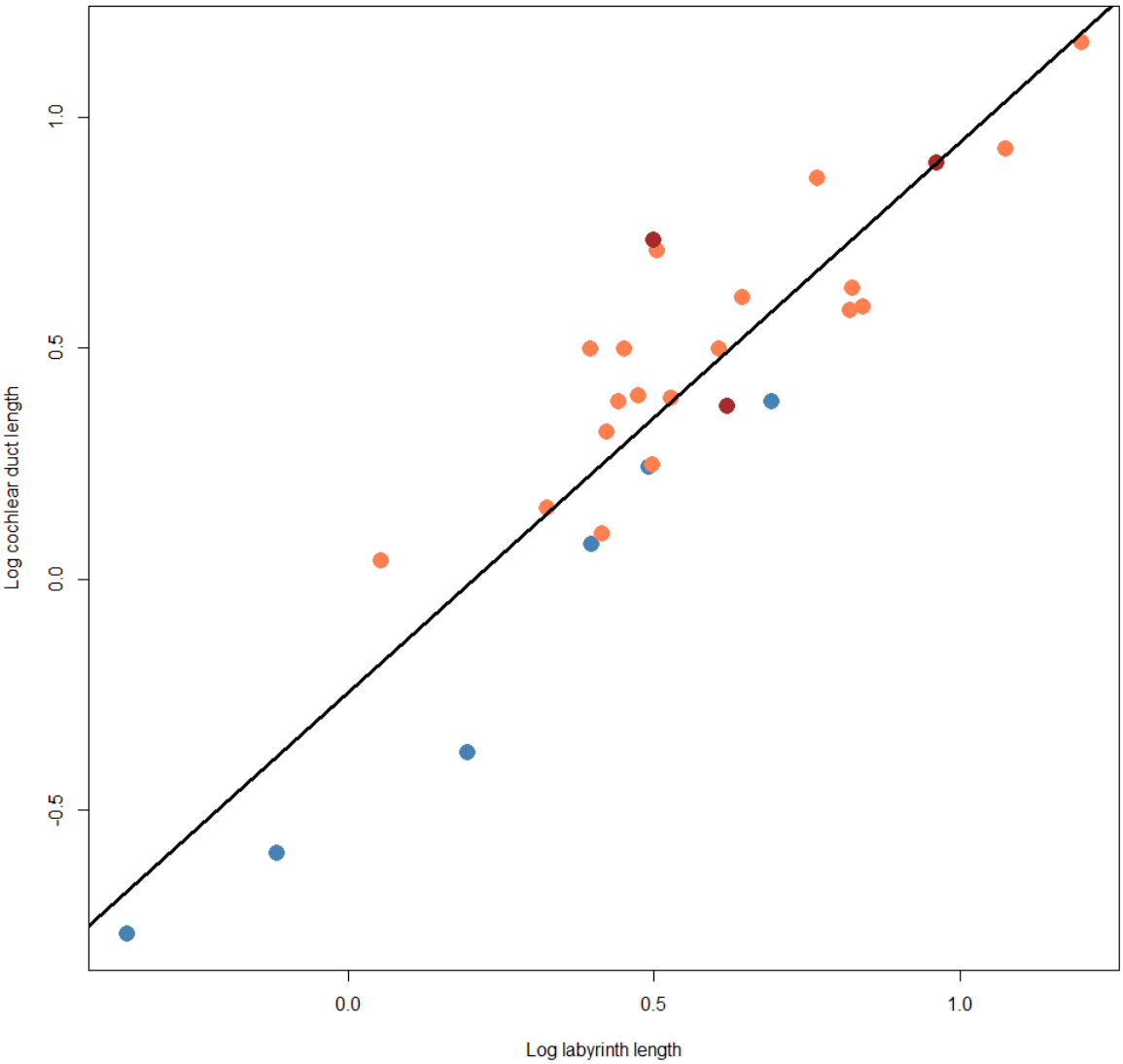

Fig. S8. Logarithmic plot of labyrinth length and cochlear duct length. Blue, pelagic; orange, semiaquatic; red, terrestrial.

13. Inclusion of *Crocodylus porosus* juvenile

The extant crocodylian *Crocodylus porosus* often ventures further offshore than other extant species. We do not include *C*. *porosus* in our dataset as the scan we acquired is of a juvenile, and we are limiting our analysis to adults. However, to demonstrate that *C*. *porosus* has an inner ear that is similar in shape to other extant crocodylians, and distinct in shape from pelagic extinct thalattosuchians, we provide an auxiliary analysis in which this juvenile specimen is included in our PCA morphospace below (analysis conducted following the same protocol as our primary PCA analysis, described above and in the main text). This demonstrates that the exclusion of *C*. *porosus* should not greatly affect our results, as its ear is exceedingly similar to the many other extant crocodylians in our dataset. We also acknowledge that extant species other than *C*. *porosus* are frequently encountered in brackish or saline environments, including one of the species in our analysis, *C*. *acutus*, and that swimming behavior in extant crocodylians appears to be the same whether an individual is in fresh or salt water. Hence, we wouldn't expect substantial differences in inner ear morphology between coastal and fluviolacustrine extant forms.

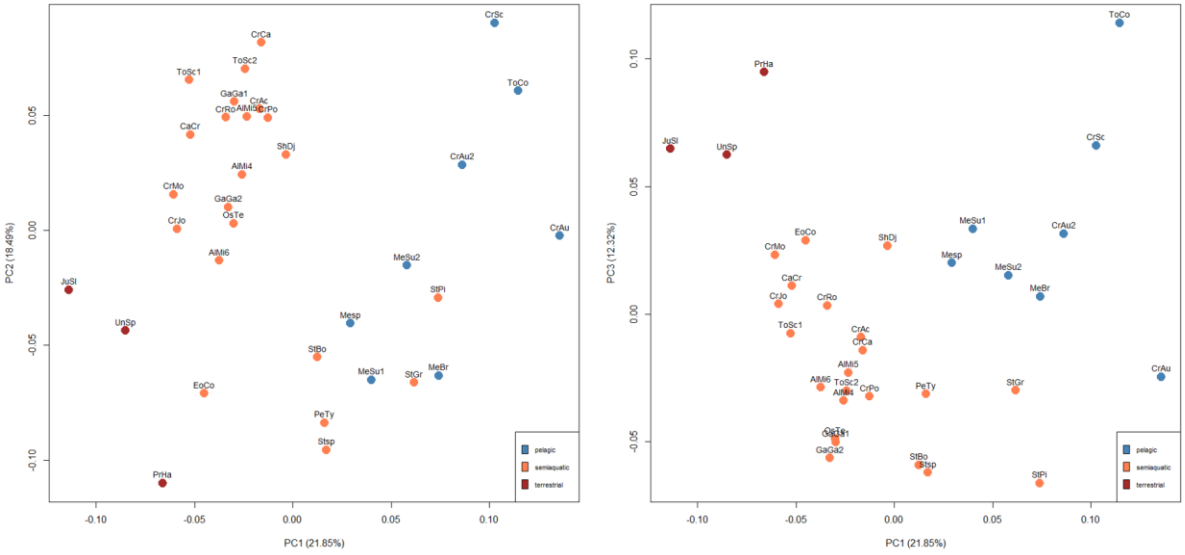

Fig. S9. PCA including the juvenile *Crocodylus porosus* (OUVC:10899; CrPo).

14. Left-Right Ear Asymmetry

To our knowledge, the only study testing whether left and right inner ear labyrinths of an archosaur are consistent in shape is a recent study of wild turkeys (24). The analyses in our paper use right labyrinths or mirrored left labyrinths. We here test whether mirrored left labyrinths resemble the shape of the right labyrinths in individuals of three key extant species, one from each major crocodilian subgroup. Importantly, we find that, for each individual, the mirrored left and actual right labyrinths fall out very close to each other in PCA morphospace (Fig. S10, analysis conducted following the same protocol as our primary PCA analysis, described above and in the main text), demonstrating that any asymmetry between left and right sides is minimal compared to the much greater amount of variation between species and between habitat groups. Thus, the inclusion of both right and mirrored left labyrinths in our dataset should not provide any serious bias. We visually show the actual left and right labyrinths of the three extant individuals in Fig. S11, which further demonstrates how similar in shape they are.

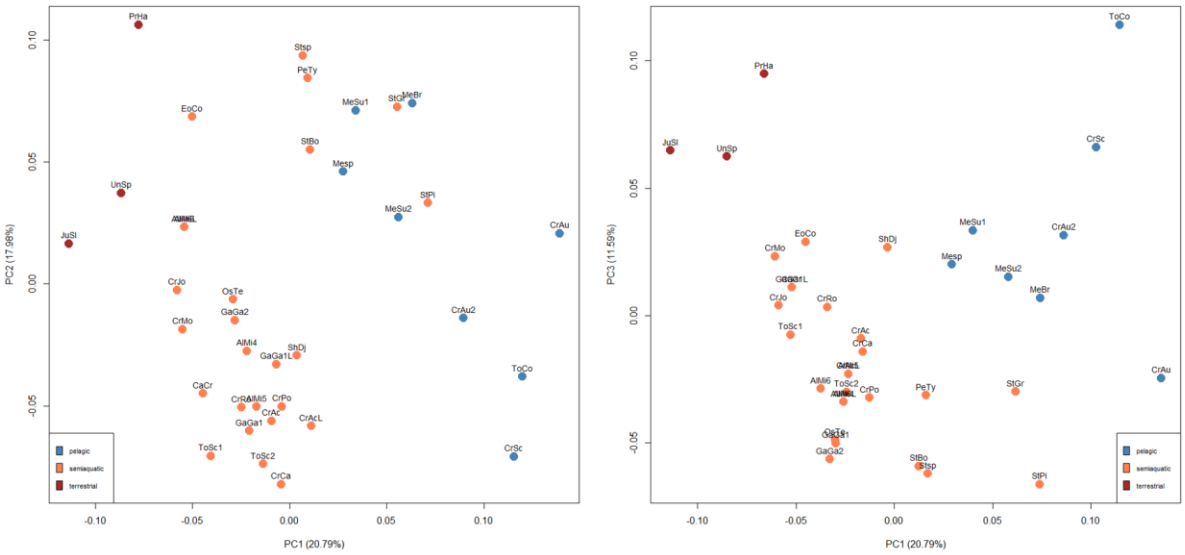

Fig. S10. PCA including the left mirrored labyrinths *for Alligator mississippiensis* (OUVC 9761; AlMi6L), *Crocodylus acutus* (FMNH 59071; CrAcL) and *Gavialis gangeticus* (TMM M-5490; GaGa1L).

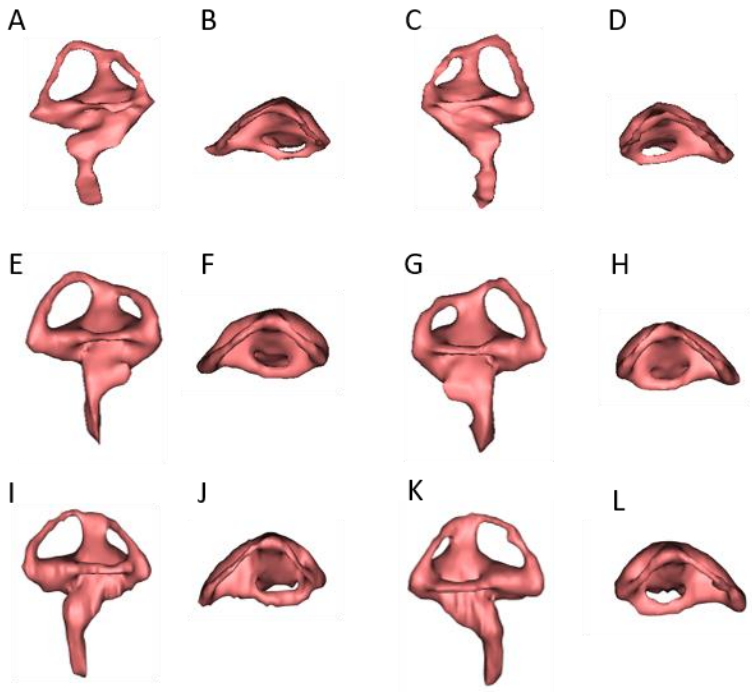

Fig. S11. Bony labyrinths of *Alligator mississippiensis* (OUVC 9761), *Crocodylus acutus* (FMNH 59071) and *Gavialis gangeticus* (TMM M-5490). A, E, I left lateral view; B, F, J left dorsal view; C, G, K right lateral view; D, H, L right dorsal view.

15. Supplementary References

1. J. M. Clark, X. Xu, C. A. Forster, Y. Wang, A Middle Jurassic ‘sphenosuchian’from China and the origin of thecrocodylian skull. *Nature* **430**, 1021–1024 (2004).

2. A. W. Crompton, K. K . Smith, “A new genus and species of crocodilian from the Kayenta Formation (Late Triassic?) of Northern Arizona” in Aspects of Vertebrate History, L. L. Jacobs, Eds. (Museum of Northern Arizona Press, Flagstaff, 1980) pp. 193–217.

3. E. H. Colbert, C. C. Mook, The Ancestral crocodilian *Protosuchus*. *Bull. Am. Mus. Nat. Hist.* **97**, 143–182 (1951).

4. F. Westphal, Die Krokodilier des Deutschen und Englischen oberen Lias. *Palaeontographica* A 116, 23–118 (1962).

5. C. W. Andrews, Descriptive Catalogue of the Marine Reptiles of the Oxford Clay: Part II (British Museum (Natural History), London, 1913).

6. Y. Herrera, M. Fernández, J. A. Varela, Morfología del miembro anterior de Geosaurus araucanensis Gasparini y Dellapé, 1976 (Crocodyliformes: Thalattosuchia). *Ameghiniana* **46**, 657–667 (2009).

7. Y. Herrera, M. S. Fernández, Z. Gasparini, Postcranial skeleton of *Cricosaurus araucanensis* (Crocodyliformes: Thalattosuchia): morphology and palaeobiological insights. *Alcheringa* ***37***, 1–14 (2013).

8. H. Karl, E. Gröning, C. Brauckmann, N. Knötschke, Revision of the genus *Enaliosuchus* Koken, 1883 (Archosauromorpha: Metriorhynchidae) from the

Early Cretaceous of northwestern Germany. *Studia Geológica Salmanticensia* **42**, 49–59 (2006).

9. M. T. Young, M.B. Andrade, S. Etches, B. L. Beatty, A new metriorhynchid crocodylomorph from the Lower Kimmeridge Clay Formation (Late Jurassic) of England, with implications for the evolution of dermatocranium ornamentation in Geosaurini. *Zool. J. Linn. Soc.* **169**, 820–848 (2013).

10. D. Pol, A. H. Turner, M. A. Norell, Morphology of the Late Cretaceous Crocodylomorph *Shamosuchus djadochtaensis* and a Discussion of Neosuchian Phylogeny as Related to the Origin of Eusuchia. *Bull. Am. Mus. Nat. Hist.* **324**, 1–103 (2009).

11. G. Grigg, D. Kirshner, *Biology and Evolution of Crocodylians* (CSIRO and Cornell University Press, 2015).

12. M. T. Young, *et al*., Convergent evolution and possible constraint in the posterodorsal retraction of the external nares in pelagic crocodylomorphs. *Zool. J. Linn. Soc.* (In press).

13. J. Ristevski, M. T. Young, M. B. Andrade, A. K. Hastings, A new species of *Anteophthalmosuchus* (Crocodylomorpha, Goniopholididae) from the Lower Cretaceous of the Isle of Wight, United Kingdom, and a review of the genus. *Cretac. Res.* **84**, 340–383 (2018).

14. A. Ősi, M. T. Young, A. Galácz, M. Rabi, A new large-bodied thalattosuchian crocodyliform from the Lower Jurassic (Toarcian) of Hungary, with further evidence of the mosaic acquisition of marine adaptations in Metriorhynchoidea. *PeerJ* **6**, e4668 (2018).

15. D. Foffa, M. M. Johnson, M. T. Young, L. Steel, S. L. Brusatte, A revision of the deep-water teleosauroid crocodylomorph *Teleosaurus megarhinus* Hulke, 1871 from the Kimmeridge Clay Formation (Late Jurassic) of England, UK. *PeerJ* **7**, e6646 (2019).

16. M. M. Johnson, M. T. Young, S. L. Brusatte, Re-description of two contemporaneous mesorostrine teleosauroids (Crocodylomorpha, Thalattosuchia) from the Bathonian of England, and insights into the early evolution of Machimosaurini. *Zoo. J. Linn. Soc.* zlz037 (2019).

17. S. Sachs, M. T. Young, P. Abel, H. Mallison, A new species of *Cricosaurus* (Thalattosuchia, Metriorhynchidae) from the Upper Jurassic of southern Germany. *Acta Palaeontologica Polonica* **64**, 345–356 (2019).

18. E. W. Wilber, What's in an Outgroup? The Impact of Outgroup Choice on the Phylogenetic Position of Thalattosuchia (Crocodylomorpha) and the Origin of Crocodyliformes. *Syst. Biol.* **64**, 624–637 (2015a).

19. E. W. Wilber, A new metriorhynchoid (Crocodylomorpha, Thalattosuchia) from the Middle Jurassic of Oregon and the evolutionary timing of marine adaptations in thalattosuchian crocodylomorphs. *J. Vert. Paleo.* 902846 (2015b).

20. E. Buffetaut, Position systématique et phylogénetique du genre Pelagosaurus Bronn, 1841 (Crocodylia, Mesosuchia), du Toarcian d'Europe. Geobios 13, 783–786 (1980).

21. J. R. Oaks, A time-calibrated species tree of crocodylia reveals a recent radiation of the true crocodiles. *Evolution* **65**, 3285–3297 (2011).

22. J. Harshman, C. J. Huddleston, J. P. Bollback, T. J. Parsons, M. J. Braun True and false gharials: a nuclear gene phylogeny of crocodylia. *Syst Biol* **52**, 386–402 (2003).

23. M. S. Y. Lee, A. M. Yates Tip-dating and homoplasy: reconciling the shallow molecular divergences of modern gharials with their long fossil record. *Proc. R. Soc*. *B* **285**, 20181071 (2018).

24. D. G. Cerio, L. M. Witmer, Intraspecific variation and symmetry of the inner-ear labyrinth in a population of wild turkeys: implications for paleontological reconstructions. PeerJ 7, e7355 (2019).